Neuropeptides 77 (2019) 101962

Contents lists available at ScienceDirect

Neuropeptides

journal homepage: www.elsevier.com/locate/npep

Hindbrain lactoprivic regulation of hypothalamic neuron transactivation and gluco-regulatory neurotransmitter expression: Impact of antecedent insulin-induced hypoglycemia

Karen P. Briski*, Santosh K. Mandal

School of Basic Pharmaceutical and Toxicological Sciences, College of Pharmacy, University of Louisiana at Monroe, Monroe, LA 71201, United States of America

ARTICLE INFO

Keywords:
Laser-catapult microdissection
Dopamine-beta hydroxylase
Fos immunocytochemistry
Antecedent insulin-induced hypoglycemia
Arcuate 382hypothalamic nucleus
Alpha-cyano-4-hydroxycinnamic acid

ABSTRACT

Hindbrain energy state shapes hypothalamic control of glucostasis. Dorsal vagal complex (DVC) L-lactate deficiency is a potent glucose-stimulatory signal that triggers neuronal transcriptional activation in key hypothalamic metabolic loci. The energy gauge AMPK is activated in DVC metabolic-sensory A2 noradrenergic neurons by hypoglycemia-associated lactoprivation, but sensor reactivity is diminished by antecedent hypoglycemia (AH). Current research addressed the premise that AH alters hindbrain lactoprivic regulation of hypothalamic metabolic transmitter function. AH did not modify reductions in A2 dopamine-beta-hydroxylase and monocarboxylate-2 (MCT2) protein expression elicited by caudal fourth ventricular delivery of the MCT inhibitor alpha-cyano-4-hydroxycinnamic acid (4CIN), but attenuated 4CIN activation of A2 AMPK. 4CIN constraint of hypothalamic norepinephrine (NE) activity was averted by AH in a site-specific manner. 4CIN induction of Fos immunolabeling in hypothalamic arcuate (ARH), ventromedial (VMN), dorsomedial (DMN) and paraventricular (PVN) nuclei and lateral hypothalamic area (LHA) was avoided by AH. AH affected reactivity of select hypothalamic metabolic neurotransmitter/enzyme marker proteins, e.g. ARH neuropeptide Y, VMN glutamate decarboxylase, DMN RFamide-related peptide-1 and -3, and LHA orexin-A profiles to 4CIN, but did not alleviate drug inhibition of ARH proopiomelanocortin. AH prevented 4CIN augmentation of circulating glucagon, but did not alter hyperglycemic or hypocorticosteronemic responses to that treatment. Results identify hindbrain lactate deficiency as a stimulus for glucagon secretion, and imply that habituation of this critical counter-regulatory hormone to recurring hypoglycemia may involve one or more hypothalamic neurotransmitters characterized here by acclimation to this critical sensory stimulus.

1. Introduction

The brain relies on a constant glucose supply to maintain vital high energy-demand nerve cell functions. Neuro-metabolic instability due to glucoprivation poses a substantial threat to brain function and well-being. Insulin-induced hypoglycemia (IIH) elicits hypothalamic activation of coordinated counter-regulatory autonomic, neuroendocrine, and behavioral functions that reverse glucose decrements. The hypothalamus is continuously apprised of cell energy imbalance by dedicated metabolic-sensory neurons in the brain that adjust synaptic firing in reaction to diminished substrate fuel supply. The hindbrain dorsal vagal complex (DVC) is a critical metabolic screening site in the brain as local deficits of the oxidizable glycolytic end-product L-lactate elevate blood glucose, whereas lactate repletion of the DVC intensifies hypoglycemia (Patil and Briski, 2005a). Caudal fourth ventricular (CV4) administration of the monocarboxylate transporter inhibitor α-cyano-4-hydroxycinnamic acid (4CIN) induces Fos protein expression, an indicator of change in cell functional status, in key hypothalamic metabolic loci. These findings verify operational connectivity of hindbrain lactoprivic-sensitive neurons with higher-order elements of the

Abbreviations: 4CIN, alpha-cyano-4-hydroxycinnamic acid; AMPK, 5′ adenosine monophosphate-activated protein kinase; ARH, arcuate hypothalamic nucleus; CV4, caudal fourth ventricle; DMN, dorsomedial hypothalamic nucleus; DMSO, dimethyl sulfoxide; DVC, dorsal vagal complex; $GAD_{65/67}$, glutamate decarboxylase$_{65/67}$; IIH, insulin-induced hypoglycemia; INS, insulin; LHA, lateral hypothalamic area; NE, norepinephrine; nNOS, neuronal nitric oxide synthase; NO, nitric oxide; NPY, neuropeptide Y; ORX-A, orexin A; pAMPK, phosphoAMPK; POMC, pro-opiomelanocortin; RFRP-1, RFamide-related peptide-1; RFRP-3, RFamide-related peptide-3; VMN, ventromedial hypothalamic nucleus

* Corresponding author at: School of Basic Pharmaceutical and Toxicological Sciences, College of Pharmacy, University of Louisiana Monroe, Monroe, LA 71291, United States of America.

E-mail address: briski@ulm.edu (K.P. Briski).

https://doi.org/10.1016/j.npep.2019.101962
Received 29 May 2019; Received in revised form 27 August 2019; Accepted 27 August 2019
Available online 28 August 2019
0143-4179/

brain gluco-regulatory network (Briski and Patil, 2005). DVC A2 noradrenergic neurons are a plausible source of lactoprivic regulatory cues as these cells express Fos during monocarboxylate transporter blockade (Patil and Briski, 2005b), and exhibit activation of the metabolic sensor 5'-AMP-activated protein kinase (AMPK) in response to hypoglycemia-associated lactoprivation, coincident with L-lactate – reversible hypoglycemic augmentation of hypothalamic norepinephrine (NE) activity (Shrestha et al., 2014).

The role of A2 metabolic sensory signaling in counter-regulatory acclimation to recurring neuroglucopenia remains unclear. Iatrogenic hypoglycemia is an incessant complication of necessary strict glycemic management of type I diabetes mellitus (T1DM). In T1DM patients, antecedent IIH (AH) often leads to hypoglycemia-associated autonomic failure (HAAF), a pathophysiological mal-adaptation that manifests as diminished hypoglycemic awareness and defective glucose counter-regulatory outflow (Cryer et al., 2003; Cryer, 2010). Animal models for recurrent insulin-induced hypoglycemia that replicate insulin delivery route, frequency of administration, and duration of action in the clinical setting reveal blunted nerve cell transcriptional activation in hypothalamic metabolic loci and the DVC in male rat brain, inferring neural habituation to repeated hypoglycemia (Paranjape and Briski, 2005; Kale et al., 2006). A2 neurons harvested by laser-catapult microdissection from male rats after induction of a single bout of hypoglycemia show decreased monocarboxylate transporter-2 (MCT2) protein expression and elevated AMPK activity (Cherian and Briski, 2011). Evidence that hypoglycemic suppression of A2 MCT2 mRNA is reversed by exogenous lactate suggests that MCT2 expression and lactate uptake into these neurons may be proportionate to extracellular lactate concentrations (Briski et al., 2009). Between recurring hypoglycemia episodes, A2 cells maintain patterns of amplified AMPK activity and diminished MCT2 protein expression; moreover, neither sensor activity nor MCT2 content varies from these adaptive baseline profiles during ensuing re-exposure to hypoglycemia (Cherian and Briski, 2011). Reports that AH prevents IIH up-regulation of A2 catecholamine biosynthetic enzyme dopamine-β-hydroxylase (DβH) mRNA (Cherian and Briski, 2011) and protein (Mandal et al., 2017) support the notion of acquired A2 nerve cell desensitization to recurring hypoglycemia.

Current research addressed the hypothesis that hindbrain lactoprivic regulatory input to the hypothalamus may acclimate to recurring hypoglycemia as a consequence of diminished A2 neuron reactivity to hypoglycemia-related lactate decrements. Here, Fos immunostaining was used as a functional mapping tool to assess whether AH causes site-specific adjustments in hypothalamic neuron transcriptional sensitivity to hindbrain lactoprivation. Tissue sections through hypothalami of male rats pretreated by daily vehicle or insulin injections ahead of intra-CV4 4CIN administration were processed for visualization of Fos labeling patterns within distinctive hypothalamic metabolic loci, e.g. arcuate (ARH), ventromedial (VMN), and dorsomedial (DMN) hypothalamic nuclei and lateral hypothalamic area (LHA). A corroborative approach involving Western blot analysis of drug treatment on expression profiles of neuropeptide/biosynthetic enzyme protein markers of metabolic neurotransmitter signaling in these structures was also implemented. Micropunch samples were evaluated by NE ELISA to address the premise that hindbrain lactoprivic-driven activity of this catecholamine transmitter in the hypothalamus habituates to AH. Additionally, combinatory immunocytochemistry/laser-catapult microdissection techniques were utilized to procure pure hindbrain A2 nerve cell samples in order to characterize 4CIN effects on A2 neuron AMPK activation and MCT2, glucose transporter, and DβH protein expression, and to determine if these cellular responses to drug treatment may be modified by AH.

2. Methods and materials

2.1. Experimental design

Adult male Sprague-Dawley rats (3–4 months of age) were maintained in groups (2–3 animals per cage) under a 14-h light/10-h dark lighting schedule (light on at 05:00 h), and allowed free access to standard laboratory rat chow (Harlan Teklad LM-485; Harlan Industries, Madison, WI, USA) and tap water. Animals were accustomed to daily handling for at least one week ahead of surgery. All protocols were conducted in accordance with NIH guidelines for care and use of laboratory animals, under ULM Institutional Animal Care and Use Committee approval. On day 1, rats were implanted with a 26-gauge stainless-steel cannula guide (prod no. C315G/SPC; Plastic One, Inc., Roanoke, VA) aimed at the caudal fourth ventricle (CV4) [Coordinates: 0 mm lateral to midline; 13.3 mm posterior to *bregma*; 6.1 mm ventral to skull surface] under ketamine/xylazine anesthesia (0.1 mL/100 g *bw ip*, 90 mg ketamine: 10 mg xylazine/mL; Henry Schein, Melville, NY) (Shrestha et al., 2014). After surgery, animals were injected intramuscularly with enrofloxacin (baytril 2.27%; 10 mg/kg) and subcutaneously (*sc*) with ketoprofen (3 mg/kg) prior to transfer individual cages. Animals were divided into three treatment groups ($n = 6$/group). On days 8–10, rats were injected *sc* at 09.00 h with sterile insulin diluent (V; Eli Lilly and Company, Indianapolis, IN) (groups 1 and 2) or neutral protamine Hagedorn insulin (INS; 12.5 U/kg bw (Paranjape and Briski, 2005) (group 3). On day 11, beginning at 09.00 h, animals were infused into the CV4 over a 30 min period with vehicle (V; 60% dimethyl sulfoxide: 40% 0.9% NaCl; group 1) or with the monocarboxylate transporter inhibitor 4CIN (50.0 μg/2.0 μL; groups 2 and 3), using a 33-gauge internal injection cannula with 0.5 mm projection (prod. no. C315I/SPC; Plastics One). Animals were sacrificed at 11.00 h for brain tissue and trunk blood collection. Dissected brains were immediately snap-frozen in liquid nitrogen-cooled isopentane and stored at −80 °C. Accuracy of cannula targeting of the CV4 was verified by visual examination of consecutive frozen tissue sections cut through the hindbrain for laser-catapult microdissection. Plasma was obtained by centrifugation and stored at −20 °C.

2.2. Preparation of hypothalamic tissue sections for Fos immunocytochemistry and micropunch dissection

From −2.00 mm to −3.20 mm posterior to *bregma*, each hypothalamus was cut into alternating series of 25 μm- or 200 μm-thick frozen sections, over repeating distances of 200 μm (8 × 25 μm sections) and 800 μm (4 × 200 μm thick sections) for Fos immunostaining (Paranjape and Briski, 2005) and tissue micropunch dissection (Vavaiya and Briski, 2007), respectively. Bilateral punches of the ARH, VMN, DMN, and LHA were removed from 200 μm-thick sections using calibrated hollow Brain Punch set tools (prod. no. 57401; Stoelting, Wood Dale, IL). Micropunched tissue from the left side of thick sections were collected into lysis buffer consisting of 2.0% sodium dodecyl sulfate, 0.05 M dithiothreitol, 10.0% glycerol, 1.0 mM EDTA, 60.0 mM Tris-HCl, pH 7.2, prior to immunoblotting. Tissue obtained from the right side of each thick section was collected into lysis buffer made of 0.01 N HCl supplemented with 1.0 mM EDTA, 4.0 mM sodium metabisulfite for ELISA analysis.

2.3. Western blot analysis of micropunch-dissected hypothalamic metabolic loci

Tissue punches were heat-denatured at 95 °C. For each protein of interest, tissue aliquots from subjects within each treatment group were pooled to create three separate sample pools per group ahead of separation on Bio-Rad Stain Free 10–12% acrylamide gels (prod. no. 161–0183; Bio-Rad, Hercules, CA), as described (Shakya et al., 2018). Gels were activated by UV light (1 min) in a Bio-Rad ChemiDoc TM Touch Imaging System before overnight transblotting (4-5 °C) to 0.45-

μm PVDF-Plus membranes (prod. no. PV4HY00010; ThermoFisherScientific, Waltham, MA). After blocking (2 h) with Tris-buffered saline, pH 7.4, containing 0.1% Tween-20 and 2% bovine serum albumin, membranes were incubated (24–48 h; 4–5^{0}C) with rabbit primary polyclonal antisera against glycogen synthase (GS; 1:2000; prod. no. 3893S; Cell Signaling Technology, Danvers, MA), glycogen phosphorylase-muscle type (GP_{MM}; 1:2000; prod. no. NBP2-16689; Novus Biologicals, Littleton, CO), glycogen phosphorylase-brain type (GP_{BB}; prod. no. NBP1-32799, 1:2000; Novus Biol.), glutamate decarboxylase$_{65/67}$ ($GAD_{65/67}$; 1:10,000; prod. no. ABN904; MilliporeSigma (Burlington, MA), neuronal nitric oxide synthase (nNOS; 1:2000; prod. no. NBP1–39681; Novus Biol.), or with a goat primary antiserum against neuropeptide Y (NPY; 1:2500; prod no. NBP1–46595; Novus Biol.). Membranes were next incubated (1 h) with goat anti-rabbit (1:5000; prod. no. NEF812001EA; PerkinElmer, Waltham, MA) or rabbit anti-goat (1:5000; prod. no. AP106P; MilliporeSigma) secondary antibodies prior to exposure to Supersignal West Femto maximum sensitivity chemiluminescent substrate (prod. no. 34096; ThermoFisherSci.). Membrane buffer washes and antibody incubations were carried out by Freedom Rocker™ Blotlbot® automation (Next Advance, Inc., Troy NY). Protein band chemiluminescence optical density (O.D.) values were obtained in the ChemiDoc MP system, and normalized to individual-lane total protein using Imagelab software (Image Lab™ 6.0.0; Bio-Rad). Precision plus protein molecular weight dual color standards (prod. no. 161–0374; Bio-Rad) were included in each Western blot analysis.

2.4. ELISA measurement of VMN, ARH, DMN, and LHA NE content

For each animal, micropunched tissue from each structure was analyzed for NE content with Noradrenaline Research ELISA™ kit reagents (Labor Diagnostika Nord GmbH & Co KG, Nordhorn, Germany), as reported (Shrestha et al., 2014).

2.5. Immunohistochemical analysis of hypothalamic Fos expression

For immunostaining was performed as previously reported (Paranjape and Briski, 2005). Briefly, 25 μm-thick sections cut at repeating rostro-caudal intervals through ARH, VMN, DMN, LHA, and paraventricular hypothalamic nucleus (PVH), and mounted on poly-L-lysine-coated glass slides. For each structure, $n = 4$ sections collected at each level were fixed with acetone prior to 60 min pre-incubation in normal goat serum (Vectastain Elite ABC HRP rabbit IgG kit; prod. no. PK-6101; Vector Laboratories, Burlingame, CA). Tissues were incubated for 48 h. (4 °C) with a rabbit polyclonal antiserum against Fos (1:250; prod. no. PC05-100 U; Millipore Sigma, Burlington, MA) diluted in TBS containing 0.05% Triton-X-100, followed by incubation with Alexa Fluor 488-conjugated anti-rabbit secondary antibodies (1:250; prod. no. A21205) for 2 h. Labeled sections were coverslipped with Vectashield antifade mounting medium (prod. no. H-1000, Vector Laboatories, Burlingame, CA), and images were captured with an LSM 5 PASCAL confocal scanning laser microscope (Carl Zeiss MicroImaging Inc., Thornwood, NY, USA). For each animal, bilateral counts of Fos-immunoreactive (−ir) neurons for each neural structures of interest were summed to establish mean tallies for each treatment group.

2.6. Western blot analysis of laser-catapult microdissected DVC A2 noradrenergic neurons

Serial 10 μm-thick frozen hindbrain sections were cut between −14.36 to −14.86 mm relative to *bregma*, and mounted on polyethylene naphthalate membrane slides (Carl Zeiss MicroImaging LLC, Thornwood, NY). Tissues were fixed with acetone, blocked with 5% normal horse serum (Vectastain Elite ABC mouse IgG kit; Vector Laboratories, Inc., Burlingame, CA), then incubated for 24 h at 4 °C with mouse monoclonal primary antibodies against tyrosine hydroxylase (TH) (1:1000; ImmunoStar, Inc., Hudson, WI). Sections were next sequentially exposed to Vectastain IgG Elite ABC mouse IgG kit biotinylated secondary antibody, ABC reagent, and Vector DAB kit reagents (Vector Laboratories) to visualize TH-immunoreactive (−ir) neurons (Briski et al., 2009). Individual TH-ir cells exhibiting a visible nucleus and complete labeling of the cytoplasmic compartment were dissected using a Zeiss P.A.L.M. UV-A microlaser (Carl Zeiss MicroImaging). For each protein of interest, triplicate pools of 50 TH-ir neuron lysates (8–9 cells per animal/per pool) were created for each treatment group and separated in Stain-Free gels, as described above. Gels were activated in a ChemiDoc MP Imaging System prior to transblotting, as described above. Membranes were pretreated with Western blotting signal enhancer (Pierce, Rockford, IL), blocked with Tris-buffer saline (TBS), pH 7.4, containing 0.1% Tween-20 (Sigma Aldrich, St. Louis, MO) and 2% bovine serum albumin (MP Biomedicals, Solon, OH), then incubated overnight at 4 °C with primary antibodies raised in rabbit against $AMPK_{\alpha1/2}$ (Thr 172; 1:2000; prod. no. 2532 s, Cell Signaling Technology, Danvers, MA), phospho$AMPK_{\alpha1/2}$ (pAMPK, Thr 172; 1:2000; prod. no. 2535; Cell Signaling Technol.), DβH (1:1000; prod. no. sc-15318; Santa Cruz Biotechnology, Inc., Santa Cruz, CA), or GLUT3 (1:1500; prod. no. NBP2-66872; Novus Biol.), or in goat against MCT2 (1:1000; prod. no. sc-14926; Santa Cruz Biotechnol.). Automated membrane buffer washes and antibody incubations were performed as described above. Membranes were incubated for 1 h with peroxidase-conjugated goat anti-rabbit (1:5000; prod. no. NEF812001EA; PerkinElmer, Boston, MA) or rabbit anti-goat (1:5000; prod. no. AP106P; EMD Millipore, Burlington, MA) secondary antisera. After exposure to SuperSignal West Femto chemiluminescent substrate, protein band O.D. signals were quantified and expressed relative to total in-lane protein using BioRad Image Lab software, as described above.

2.7. Blood analyte measurements

Plasma glucose levels were measured using an Accu-Check Aviva Plus glucometer (Roche Diagnostics, Indianapolis, IN), as described (Kale et al., 2006). Plasma corticosterone (ADI-900-097; Enzo Life Sciences, Inc., Farmingdale, NY) and glucagon (EZGLU-30 K, EMD Millipore, Billerica, MA) concentrations were determined using commercial ELISA kit reagents (Alhamami et al., 2018a, 2018b).

2.8. Statistical analyses

Mean circulating glucose, corticosterone, and glucagon concentrations, normalized Western blot protein O.D. values, and tissue NE content levels were evaluated between treatment groups by one-way analysis of variance and Student Newman Keuls *post-hoc* test. Differences of $p < .05$ were considered significant.

3. Results

Laser-catapult microdissected A2 neuron samples were analyzed by Western blot to investigate whether AH modifies cellular nutrient transporter and AMPK responses to hindbrain lactate deficiency. As shown in Fig. 1, A2 DBH protein content was down-regulated by 4CIN (Panel A) [V/4CIN versus V/V; $F_{(2,6)} = 7.20$; $p = .02$]; this inhibitory response to drug treatment was unaffected by AH. Data in Panels B-D indicate that MCT2 [$F_{(2,6)} = 10.78$; $p = .01$] and GLUT3 [$F_{(2,6)} = 11.00$; $p = .004$] expression profiles were significantly reduced, whereas GLUT4 content was enhanced [$F_{(2,6)} = 7.03$; $p = .02$] by hindbrain monocarboxylate transporter inhibition in both hypoglycemia-naïve and AH-pretreated animals [V/4CIN and AH/4CIN versus V/V]. 4CIN suppressed total AMPK [Panel E; $F_{(2,6)} = 16.74$; $p < .0001$] and pAMPK [Panel F; $F_{(2,6)} = 12.87$; $p = .0002$] protein levels in A2 neurons. AH did not affect the A2 total AMPK response to drug treatment, but resulted in a relatively greater magnitude of suppression of pAMPK expression due to 4CIN [AH/4CIN versus V/4CIN].

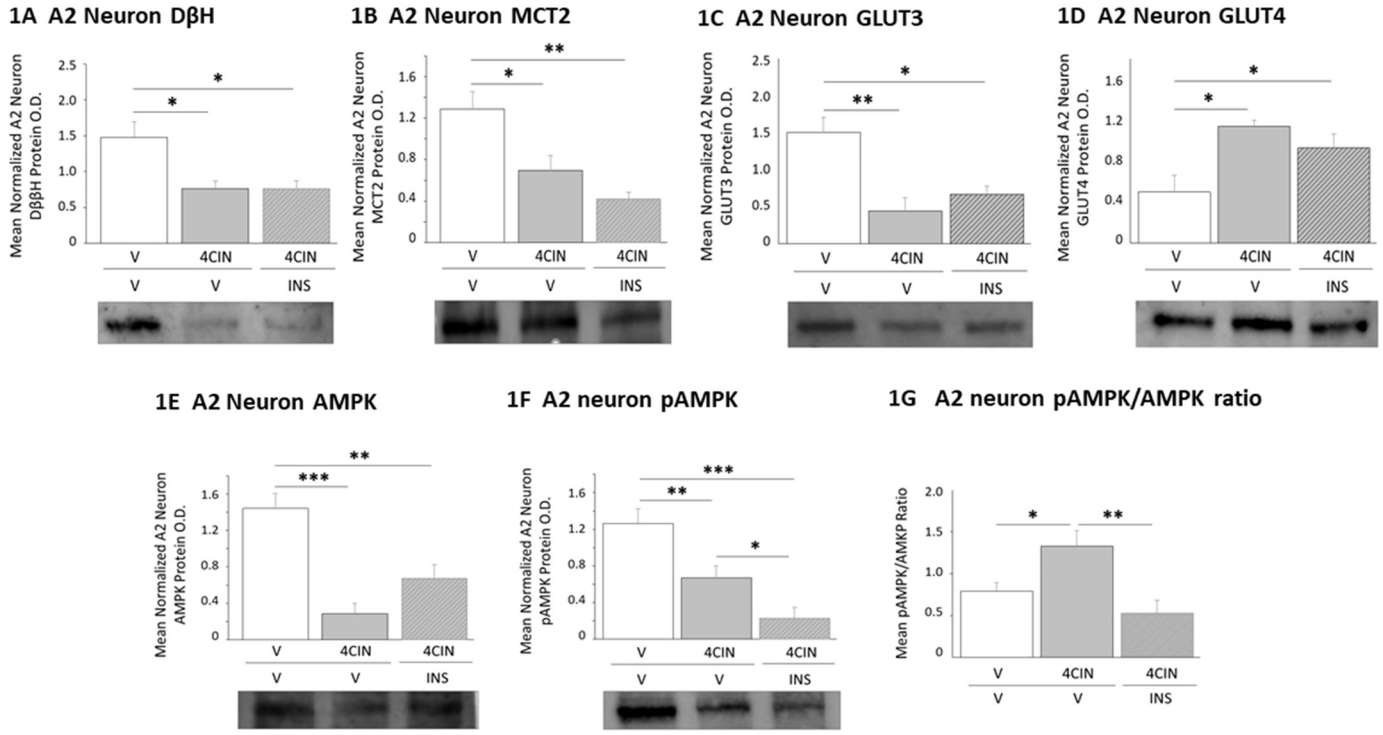

Fig. 1. Antecedent Insulin-Induced Hypoglycemia (AH) Regulation of Dorsal Vagal Complex A2 Noradrenergic Nerve Cell Dopamine-Beta-Hydroxylase (DβH) and Nutrient Transporter Expression and 5′-AMP-Activated Protein Kinase (AMPK) Activation in Response to Caudal Fourth Ventricular (CV4) Administration of the Monocarboxylate Transporter Inhibitor Alpha-Cyano-4-Hydroxycinnamic Acid (4CIN). Lysates from laser-catapult microdissected tyrosine hydroxylase-immunopositive A2 neurons were pooled within treatment groups: Group 1 (V/V; solid white bars; $n = 6$): daily subcutaneous (*sc*) vehicle (V; sterile insulin diluent) injection prior to intra-CV4 infusion of vehicle (V; dimethyl sulfoxide:NaCl); Group 2 (V/4CIN; solid gray bars; n = 6): daily *sc* V injections followed by CV4 4CIN; Group 3 [INS/4CIN; diagonal-striped gray bars; n = 6): daily *sc* insulin (INS) injections followed by CV4 4CIN] for Western blot analysis. Data depict mean normalized protein optical density (O.D) measures ± S.E.M. of A2 cell DβH (Panel A), monocarboxylate transporter-2 (MCT2; Panel B), glucose transporter-3 (GLUT3; Panel C), glucose transporter-4 (GLUT4; Panel D), AMPK (Panel E), and phosphoAMPK (pAMPK; Panel F) protein expression in each treatment group. *$p < .05$; **$p < .01$; ***$p < .001$.

The mean ratio of pAMPK/AMPK expression in A2 neurons was significantly increased by 4CIN, a response that was averted by AH [Panel G; $F_{(2,6)} = 6.98$; $p = .009$].

Data presented in Table 1 show that 4CIN administration significantly increased mean numbers of Fos-ir neurons in each neural structure evaluated, e.g., ARH, VMN, DMN, LHA, and PVH [V/4CIN versus V/V]. AH normalized patterns of Fos labeling in the VMN, LHA, and PVH of 4CIN-treated animals, and attenuated this expression in the ARH and DMN. Fig. 2 depicts representative patterns of Fos immunostaining for V/V, V/4CIN, and AH/4CIN treatment groups in the DMN (Row 1; Panels A.1 – A.3) and VMN (Row 2; Panels B.1 – B.3).

ARH NPY acts centrally to regulate circulating insulin, glucagon, and corticosterone levels (Marks and Waite, 1997; Parikh and Marks, 1997) and to modulate insulin control of hepatic glucose production (van den Hoek et al., 2004). ARH POMC is a catabolic neuropeptide that is stimulated by nutrient, neurochemical, and endocrine (leptin, insulin) surrogates of energy sufficiency (Wardlaw, 2011). POMC is processed to yield distinct bio-active peptide products that exert divergent effects on feeding, e.g. anorexigenic alpha-melanocyte-stimulating hormone (α-MSH) and orexigenic beta-endorphin (β-END)

Table 1
Effects of Antecedent Insulin-Induced Hypoglycemia (AH) on Alpha-cyano-4-hydroxycinnamic acid (4CIN) Induction of Fos Immunoreactivity in Hypothalamic Glucoregulatory Structures.

	Treatment groups		
	V/V[a]	V/4CIN[b]	AH/4CIN[c]
	Mean counts of Fos-immunoreactive neurons ± S.E.M.[d]		
Arcuate hypothalamic nucleus (nuc.)	27.4 ± 3.6	86.0 ± 4.7*	45.6 ± 4.5*,**
Ventromedial hypothalamic nuc.	31.6 ± 2.8	80.0 ± 40*	42.4 + 3.0**
Dorsomedial hypothalamic nuc.	23.0 ± 3.5	96.6 ± 4.8*	48.0 + 5.4*,**
Lateral hypothalamic area	31.0 ± 5.3	59.2 ± 4.8*	23.6 + 3.0**
Paraventricular hypothalamic nuc.	36.0 ± 3.0	102.4 ± 5.9*	46.0 + 4.3**

*p < .05 compared to V/V.
**p < .05, compared to V/4CIN.
[a] Subcutaneous (*sc*) vehicle (V) injection once per day over 3 consecutive days, followed by vehicle (V) infusion into caudal fourth ventricle (CV4) on day 4.
[b] *sc* V injection once per day over 3 days, followed by CV4 4CIN infusion on day 4.
[c] *sc* 12.5 U neutral protamine Hagedorn insulin injection once per day over 3 days (AH), followed by CV4 4CIN infusion on day 4.
[d] n = 6 animals/group.

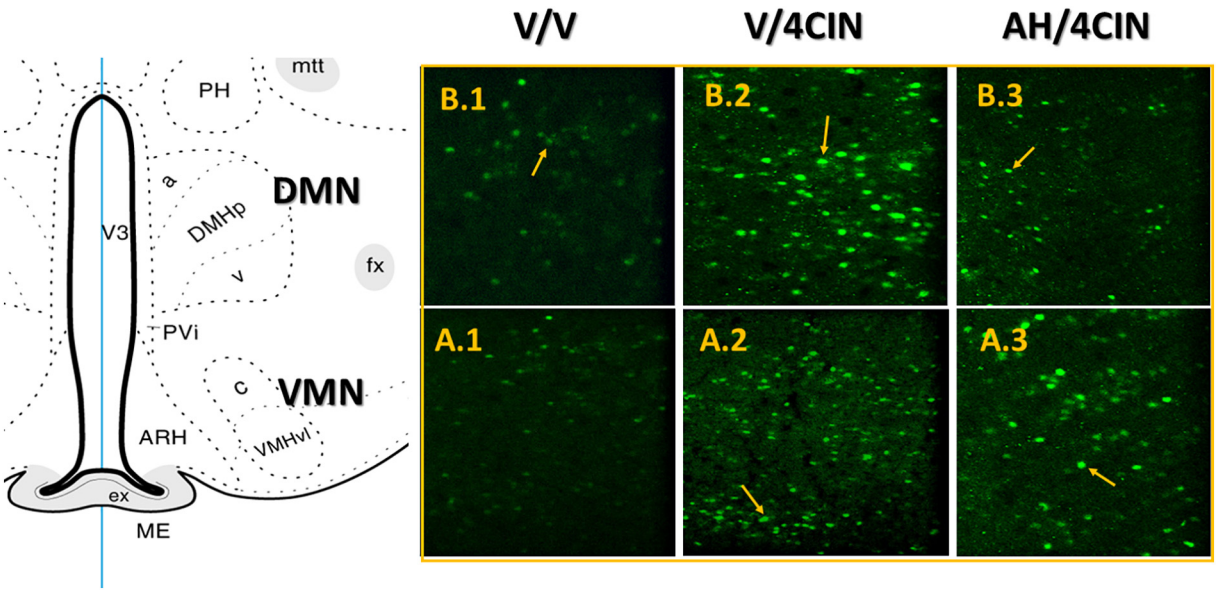

Fig. 2. AH Effects on 4CIN Induction of Hypothalamic Fos Immunoreactivity. Data show representative patterns of Fos immunolabeling in the DMN (upper row; Panels A.1 – A.3) and VMN (lower row; Panels B.1 – B.3) in animals in V/V (left-hand column), V/4CIN (middle column), and AH/4CIN (right-hand column) treatment groups. Yellow arrows denote Fos-ir-positive neuronal nuclei. The illustration of the mediobasal hypothalamus denotes respective locations of the DMN and VMN relative to distinctive landmarks, e.g. third ventricle (V3) and median eminence (ME). Scale bars: 80 µm. Abbreviations: ARH, arcuate hypothalamic nucleus; PVi, intermediate periventricular nucleus; MEex, median eminence, external lamina; fx, fornix; PH, posterior hypothalamic nucleus; mtt, mamillothalamic tract; DMHa,p,v, dorsomedial hypothalamic nucleus anterior, posterior, ventral parts; VMHc,vl, ventromedial hypothalamic nucleus central, ventrolateral parts. (For interpretation of the references to color in this figure legend, the reader is referred to the web version of this article.)

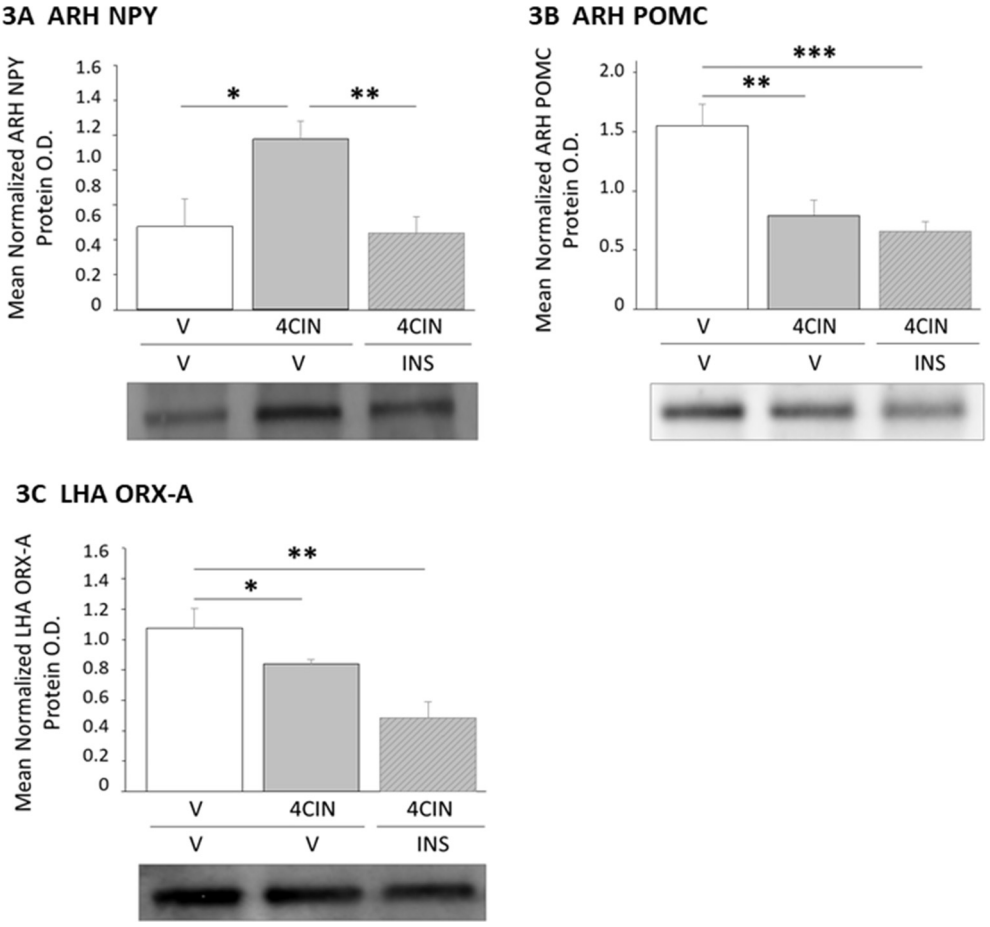

Fig. 3. AH Regulation of ARH Neuropeptide Y (NPY) and Proopiomelanocortin (POMC) Protein Expression in 4CIN-Treated Rats. Results depict mean normalized ARH NPY (Panel A) and POMC (Panel B) O.D. measures ± S.E.M. in groups of male rats given daily sc V injections prior to intra-CV4 V (V/V) or 4CIN (V/4CIN) administration or injected daily with INS prior to intra-CV4 4CIN (INS/4CIN). $*p < .05$; $**p < .01$; $***p < .001$.

(Vergoni and Bertolini, 2000; Silva et al., 2001). β-END facilitates glucose counter-regulation by stimulation of adrenomedullary epinephrine and NE secretion (Van Loon and Appel, 1980; Van Loon et al., 1981). Here, we investigated whether NPY and/or POMC expression is regulated by hindbrain lactoprivation, and if such control is modified by AH. Data in Fig. 3 depict effects of hindbrain 4CIN administration on ARH NPY (Panel A) and POMC (Panel B) protein content in non-AH- versus AH-exposed rats. 4CIN delivery to hypoglycemia-naïve rats caused significant up-regulation of NPY protein content [V/4CIN versus V/V; $F_{(2,6)} = 6.67$; $p = .006$]; animals given daily insulin injections prior to 4CIN exhibited no change in this profile versus controls [INS/4CIN versus V/V]. 4CIN suppressed ARH POMC protein levels to an equivalent extent in AH and non-AH groups [$F_{(2,6)} = 12.09$; $p = .0005$]. The LHA orexigenic neuropeptide ORX-A promotes hyperphagia and hyperglycemia (Sakurai et al., 1998; Yi et al., 2009). Current results (Fig. 2, Panel C) indicate that this protein profile is inhibited by hindbrain lactoprivation [V/4CIN versus V/V; $F_{(2,6)} = 9.33$; $p = .006$], and that AH exposure caused amplification of this negative response to 4CIN [INS/4CIN versus V/4CIN].

VMN nitric oxide (NO) and γ-aminobutyric acid (GABA) neurons respectively stimulate or inhibit counter-regulatory hormone secretion (Chan and Sherwin, 2013), and are sensitive to NE-controlled provision of L-lactate derived from glucosyl monomers of astrocyte glycogen (Alhamami et al., 2018b; Mahmood et al., 2019). Studies here examined whether VMN gluco-regulatory signaling responses to 4CIN correlate with adjustments in VMN astrocyte glycogen metabolic enzyme protein expression, and if AH influences drug effects on these neuronal and astrocyte protein profiles. Data presented in Fig. 4 Panels A and B illustrate significant 4CIN suppression of the enzyme protein marker nNOS [$F_{(2,6)} = 5.43$; $p = .02$] alongside augmentation of VMN $GAD_{65/67}$ content [$F_{(2,6)} = 9.37$; $p = .001$]. AH prevented 4CIN up-regulation of $GAD_{65/67}$, but did not modify drug suppression of nNOS expression. Glycogen metabolism is controlled by opposing actions of GS and GP, which catalyze glycogen synthesis and degradation, respectively. Data here indicate that hindbrain monocarboxylate transporter blockade causes AH-reversible stimulation of VMN GS expression (Fig. 4, Panel C) [$F_{(2,6)} = 15.20$; $p = .005$]. 4CIN administration inhibited the NE-sensitive GP variant GP_{MM} (Müller et al., 2015; Nadeau et al., 2018) in both hypoglycemia-naïve and AH-pretreated animals [Panel 4D; $F_{(2,6)} = 49.63$; $p = .0002$]. In contrast, data in Fig. 4, Panel E show that 4CIN increased expression of energy deficit-sensitive GP variant VMN GP_{BB}, and that this stimulatory drug effect was prevented by AH [$F_{(2,6)} = 17.11$; $p = .003$].

The DMN peptide RF-amide-related peptide-3 (RFRP-3), the mammalian gonadotropin-inhibitory hormone ortholog, inhibits reproductive neuroendocrine function in females (Hu et al., 2019) and regulates feeding and glucostasis in males (Leon et al., 2014). Effects of the structurally-related RFRP-1 variant on these parameters is less clear. As shown in Fig. 5, hindbrain lactoprivation significantly suppressed RFRP-1 (Panel A) [$F_{(2,6)} = 13.60$; $p = .0008$], but did not alter RFPR-3 levels (Panel B) [$F_{(2,6)} = 6.38$; $p = .03$] in the male DMN. AH pretreatment normalized RFRP-1 and up-regulated RFRP-3 expression in 4CIN-treated animals [INS/4CIN versus V/4CIN].

Current studies evaluated 4CIN effects on site-distinctive NE activity to address the premise that AH may influence patterns of hypothalamic catecholamine activity triggered by hindbrain lactate deficiency. Data illustrated in Fig. 6 show that 4CIN significantly decreased NE content in ARH [$F_{(2,15)} = 67.25$; $p < .0001$], VMN [$F_{(2,15)} = 98.13$; $p < .0001$], DMN [$F_{(2,15)} = 217.6$; $p < .0001$], and LHA [$F_{(2,15)} = 58.41$; $p < .0001$] micropunch tissue samples. Drug-associated reductions in NE activity were unaffected by AH, except in the LHA where NE levels were relatively higher in INS/4CIN versus V/4CIN rats.

Data illustrated in Fig. 7 show that 4CIN elevated plasma glucose levels (Panel A) [$F_{(2,15)} = 13.92$; $p = .001$], and that this positive response was unaffected by AH. Drug treatment caused divergent changes in circulating glucagon (Panel B) [$F_{(2,15)} = 7.36$; $p = .02$] and corticosterone (Panel C) [$F_{(2,15)} = 90.69$; $p < .0001$] concentrations. AH prevented 4CIN-induced augmentation of glucagon secretion, but did not modify patterns of corticosterone secretion in drug-treated animals.

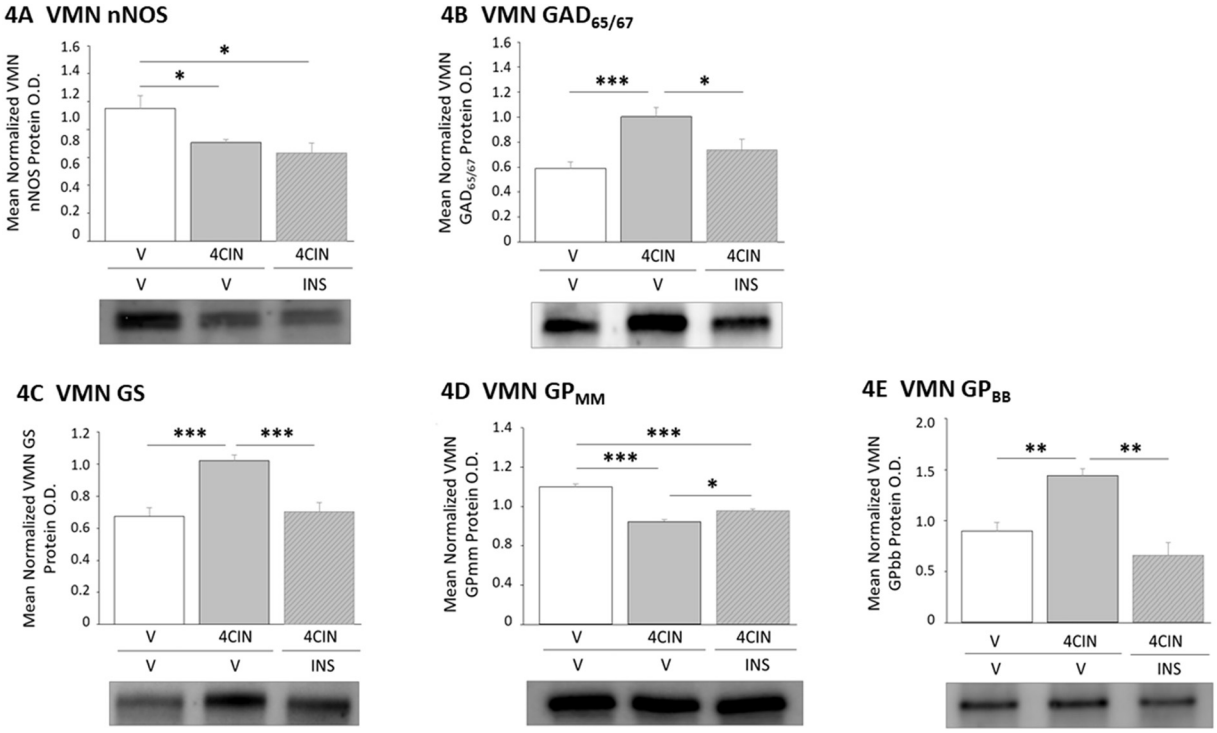

Fig. 4. 4CIN-Associated Patterns of VMN Neuronal Nitric Oxide Synthase (nNOS), Glutamate Decarboxylate$_{65/67}$ ($GAD_{65/67}$), Glycogen Synthase (GS), and Glycogen Phosphorylase (GP) Protein Expression; Impact of AH. Results show mean normalized VMN nNOS (Panel A), $GAD_{65/67}$ (Panel B), GP (Panel C), GP-muscle type (GP_{MM}; Panel D) and GP-brain type (GP_{BB}; Panel E) O.D. values ± S.E.M. for V/V, V/4CIN, and INS/4CIN treatment groups. *$p < .05$; **$p < .01$; ***$p < .001$.

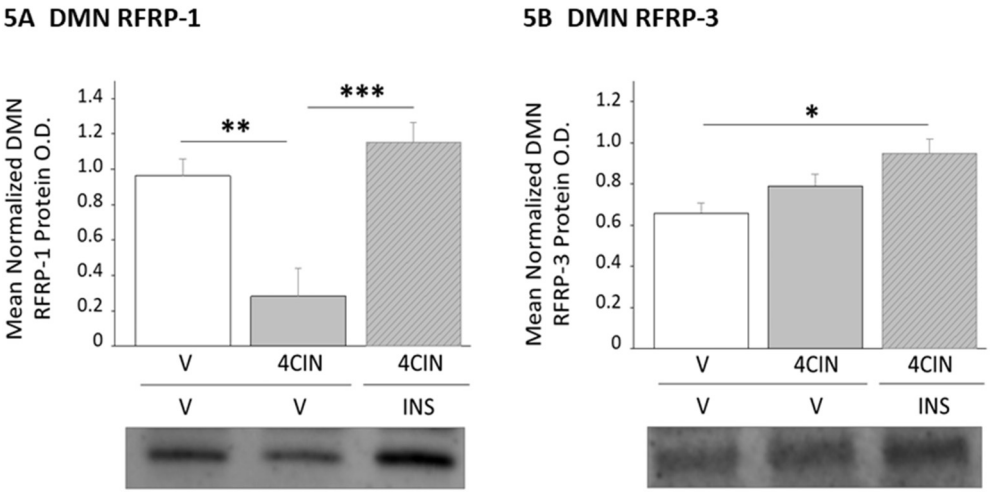

Fig. 5. AH Regulation of DMN RFamide-Related Peptide-1 (RFRP-1) and − 3 (RFRP-3) Protein Responses to 4CIN. Data illustrate indicate mean normalized DMN RFRP-1 (Panel A) and RFRP-3 (Panel B) O.D. measures ± S.E.M. for V/V, V/4CIN, and INS/4CIN treatment groups. *$p < .05$; **$p < .01$; ***$p < .001$.

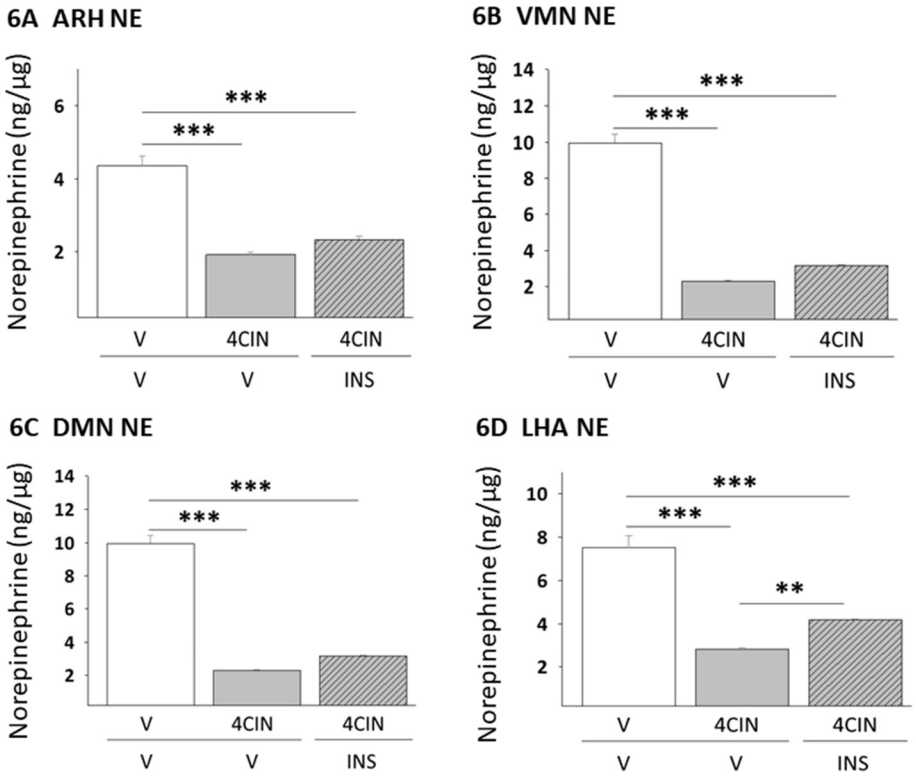

Fig. 6. AH Regulation of 4CIN-Associated Patterns of Hypothalamic Norepinephrine (NE) Activity. Results depict mean ARH (Panel A), VMN (Panel B), DMN (Panel C), and LHA (Panel D) NE tissue content ± S.E.M. for V/V, V/4CIN, and INS/4CIN treatment groups. *$p < .05$; **$p < .01$; ***$p < .001$.

4. Discussion

Current research investigated whether AH alters hindbrain lactoprivic regulation of hypothalamic nerve cell transcriptional activity and metabolic neurotransmitter signaling in male rats. Results show that AH reduced intra-CV4 4CIN induction of hypothalamic Fos immunoreactivity, and may normalize (ARH NPY; VMN GABA) or modify (LHA ORX-A; DMN RFRP) treatment effects on select hypothalamic metabolic neurotransmitters. AH did not modify drug suppression of A2 nerve cell noradrenergic transmission and hypothalamic NE activity, but attenuated A2 AMPK activation by 4CIN. These findings imply that AH may modify hindbrain lactoprivic control of hypothalamic motor outflow via adjustments in non-catecholamine cues from A2 cells and/or hypothalamic target reactivity to lactoprivic-driven NE input. Data identify hindbrain energy fuel status as a stimulus for glucagon secretion, and suggest that habituation of this critical counter-regulatory hormone to recurring hypoglycemia may involve one or more hindbrain lactoprivic-sensitive hypothalamic neurotransmitters identified here. Present outcomes bolster the notion of hindbrain involvement in brain gluco-regulatory network acclimation to recurring hypoglycemia.

Western blot analyses of microdissected DVC A2 neuron samples showed that expression of the catecholamine biosynthetic enzyme DβH was diminished 2 h after initiation of 4CIN infusion, inferring that cellular noradrenergic transmission may correspondingly fall below baseline at this specific time point. Intriguingly, this protein is up-regulated in A2 cells following one hour of hypoglycemia (Mandal and

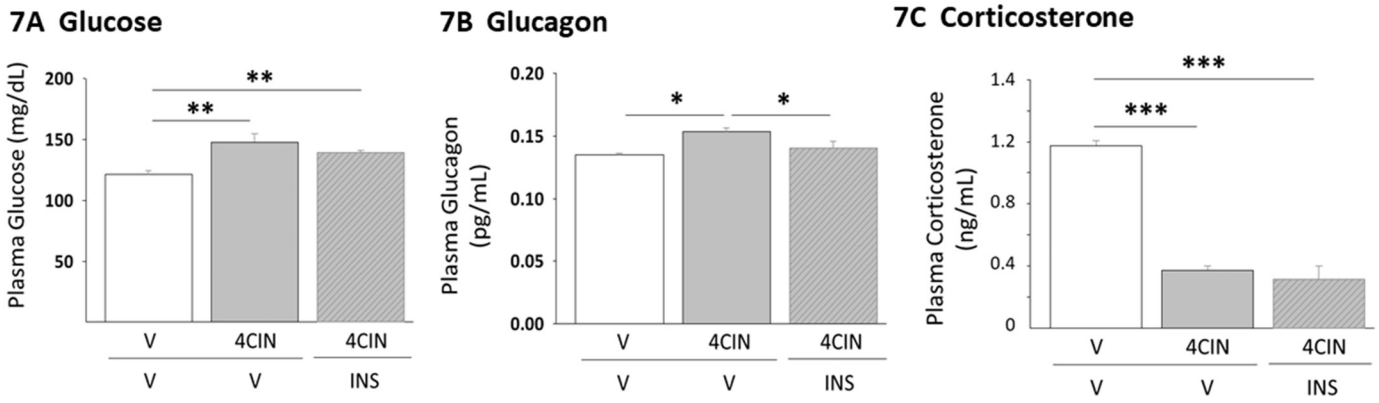

Fig. 7. Effects of Intra-CV4 4CIN Administration on Circulating Glucose, Glucagon, and Corticosterone Concentrations; Impact of AH. Results depict circulating glucose (Panel A), glucagon (Panel B), and corticosterone (Panel C) levels + S.E.M. for groups of V/V, V/4CIN, and INS/4CIN treatment groups. $*p < .05$; $**p < .01$; $***p < .001$.

Briski, 2018). As these studies utilized different treatment paradigms, including choice of drug and its route of administration, and evaluated protein expression at disparate time intervals after drug delivery, it is unclear if DβH expression is elevated by 4CIN at +1 h, then subsequently decreased in accordance with a biphasic response pattern. We speculate that A2 NE signaling may vary in magnitude and/or duration after *icv* 4CIN versus peripheral insulin injection as the former paradigm exposes these cells to a singular stimulus of decreased lactate uptake, whereas A2 neurons likely integrate a broader array of cues associated with systemic hypoglycemia, including local as well as brain-wide reductions in extracellular lactate and glucose. Moreover, A2 reactivity to local, pharmacological lactoprivation may be tempered by 4CIN-induced hyperglycemia (Patil and Briski, 2005a, 2005b). Hypoglycemia-naïve and AH-exposed animals exhibited equivalent A2 DβH profiles after 4CIN administration, implying that aside from the prospect that this protein profile may diverge between these experimental groups earlier than +2 h, DβH expression may be controlled principally by current substrate availability and thus unaffected by AH. Current evidence that 4CIN suppressed MCT2 and GLUT3 profiles, but up-regulated GLUT4 expression implies that A2 neurons may react to local lactoprivation by increasing their reliance upon glucose as an energy substrate; moreover, data reveal that this response is refractory to AH. Outcomes here affirm the notion that A2 MCT2 expression is proportionate to lactate uptake and that hypoglycemic reductions in this protein profile (Cherian and Briski, 2011) may reflect, in part, diminished availability of this distinct substrate fuel.

Data reveal that 4CIN treatment reduced total AMPK and pAMPK protein expression in A2 neurons. Despite drug-associated augmentation of the pAMPK/AMPK ratio, net sensor activity is presumably reduced owing to down-regulated pAMPK levels. We previously reported that hypoglycemia stimulates A2 pAMPK profiles (Cherian and Briski, 2011). Differential outcomes here may reflect, in part, divergent A2 sensor responsiveness to singular suppression of local monocarboxylate transporter function versus systemic glucose deficiency, which is likely to affect afferent input to A2 neurons from other metabolic-sensory cells located in the CNS and/or periphery. The significant decline in pAMPK profiles in AH- versus hypoglycemia-naïve animals injected with 4CIN infers that drug-associated patterns of sensor activation are diminished by prior exposure to hypoglycemia.

Present data align with earlier reports that 4CIN action within the caudal hindbrain intensifies hypothalamic Fos immunostaining patterns (Briski and Patil, 2005), and provide novel proof that drug-associated counts of Fos-ir neurons in each metabolic structure were significantly reduced by AH pretreatment. This functional mapping strategy demonstrates overall impedance of neuronal transcriptional reactivity to hindbrain lactoprivation in those loci by recurring hypoglycemia. As the neural structures examined here oversee multiple physiological and behavioral activities, outcomes here provide a useful neuroanatomical foundation for assessment of individual neurotransmitter reactivity to singular versus recurring exposure to this hindbrain stimulus and the functional sequelae of habituated transmission of those neurochemicals, namely changes in gluco-regulatory and/or non-metabolic motor outflow. Although inducible Fos immuno-expression is a reliable sign of altered cell functionality, activation of this proto-oncogene is not a definitive nor automatic sign of change in neuronal firing rate. Thus, it is plausible that one or more bouts of hypoglycemia-associated hindbrain lactoprivation may affect genomic activity that is unrelated to neurotransmission, namely substrate fuel utilization and energy partitioning and expenditure.

Efforts to clarify hindbrain lactoprivic regulation of characterized hypothalamic metabolic transmitter signaling were started here using Western blot techniques to measure marker protein profiles in micropunch-dissected hypothalamic tissue. Pharmacological inhibition of hindbrain monocarboxylate transport produced opposite changes in expression profiles of the ARH anabolic neurotransmitter NPY (up-regulated) versus catabolic POMC (down-regulated). It should be noted that demonstrable changes in tissue neurotransmitter content do not constitute definitive evidence for either up- or down-regulated protein expression. Evaluation of effects of reduced transmitter accumulation on neuronal signaling would require analysis of transmitter turnover, namely the ratio of synthesis/metabolism/release/exocytosis, unfortunately, such methodology is not currently available. It is also acknowledged that measures of site-specific hypothalamic transmitter peptides may vary between distinctive time points after drug delivery. Current work did not address whether hindbrain lactate status govern post-translational yield of bioactive α-MSH and/or β-END from the parent POMC molecule. Since hypoglycemia potently stimulates NPY (Alhamami et al., 2018a, 2018b; Mandal and Briski, 2018), current findings suggest that hindbrain lactoprivation may be a critical sensory stimulus to these anabolic neurons during systemic metabolic shortfall. We observed that POMC expression does not change or is diminished during hypoglycemia according to insulin dosage (Alhamami et al., 2018a, 2018b), results that imply that lactate deficit input to these cells may be counter-balanced by stimulatory cues at higher exposure to insulin. As AH prevented NPY, but not POMC reactivity to 4CIN, pre-exposure to hypoglycemia may differentially control volume (e.g. magnitude) and/or neurochemical composition of hindbrain lactoprivic signals to these distinctive metabolic nerve cell groups, or alternatively, result in dissimilar changes in receptivity of NPY versus POMC neurons to that particular stimulus or other incoming cues. These results suggest that recurring hypoglycemia may blunt hindbrain lactoprivic stimulation of ARH anabolic signaling, but not suppression of catabolic cues.

It was predicted that hindbrain lactoprivation would suppress the VMN gluco-inhibitory stimulus GABA and increase gluco-stimulatory

NO signaling; however current data instead show that VMN $GAD_{65/67}$ and nNOS proteins were up- or down-regulated, respectively, by 4CIN. We reported that intra-VMN NE administration elicits comparable adjustments in these protein profiles (Ibrahim et al., 2019), consistent with observations that NE stimulates GABA signaling (Beverly et al., 2000). 4CIN-associated patterns of $GAD_{65/67}$ and nNOS expression may reflect positive NE effects on VMN metabolic-sensory monitoring of local and/or systemic gauges of energy stability. VMN $GAD_{65/67}$ expression in hypoglycemic male rats is augmented by delivery of the GP inhibitor 1,4-dideoxy-1,4-imino-d-arabinitol (DAB) into that structure (Alhamami et al., 2018b). Since NE inhibits VMN GP_{MM} expression (Ibrahim et al., 2019), current evidence for 4CIN inhibition of this protein raises the prospect of a regulatory connection between glycogen metabolism and $GAD_{65/67}$, namely that GABA neurons may interpret attenuated NE-driven glycogen breakdown and coincident glycogen mass augmentation, owing to 4CIN up-regulation of GS expression, as an indicator of increased energy reserves. On the other hand, 4CIN increased VMN GP_{BB} profiles, suggesting that hindbrain lactoprivation may enhance energy deficit-associated glycogenolysis in this structure. AH prevented VMN GS, $GAD_{65/67}$, and GP_{BB}, but not GP_{MM} protein responses to 4CIN. These data suggest that averted effects of 4CIN on VMN GABA signaling may reflect, in part, a net reduction in drug-associated augmentation of glycogen mass. Our assumption was that LHA tissue ORX-A protein content would be up-regulated by 4CIN, but results indicate that drug treatment suppressed this profile. Present outcomes align with evidence that neurotoxic destruction of the dorsomedial hindbrain increased LHA ORX-A levels in an insulin dosage-dependent manner in hypoglycemic male rats (Alhamami et al., 2018a), as well as reports that direct application of NE to LHA tissue in vitro suppresses ORX nerve cell electrical activity (Yamanaka et al., 2006).

Current studies provide unique proof of differential sensitivity of hindbrain lactoprivic control of DMN RFRP-1 and -3 to AH. Here, 4CIN treatment significantly decreased RFRP-1 expression, but did not affect RFRP-3 tissue content. These findings contrast with observations that IIH increases RFRP-1 and reduces RFRP-3 levels in these animals (Mandal and Briski, 2018), suggesting that the impact of this hindbrain stimulus on these proteins is apparently mitigated by other regulatory cues during hypoglycemia. Hypoglycemia-exposed animals exhibited normalized RFRP-1 protein levels after 4CIN administration. The relevance of AH-associated desensitization of RFRP-1 reactivity to lactoprivic signaling to glucose glucose counter-regulation is unclear at present. On the other hand, AH caused augmented RFRP-3 reactivity to 4CIN, implying that neurotransmitter sensitivity to this hindbrain regulatory cue may increase. Again, further work is needed to characterize the impact of this positive adaptation on gluco-regulation during recurring hypoglycemia.

Hindbrain 4CIN administration decreased tissue NE levels in all hypothalamic metabolic structures examined here, coincident with drug suppression of A2 neuron DβH protein expression. This outcome contrasts with reports of heightened hypothalamic NE content following a similar time frame after onset of IIH (Shrestha et al., 2014). As the present study did not evaluate NE activity at multiple intervals after 4CIN delivery, it is unclear if lactoprivic-driven noradrenergic input to the hypothalamus follows a biphasic pattern after hindbrain monocarboxylate transport blockade in the absence of systemic hypoglycemia, and if diminished hypothalamic noradrenergic activity seen here at +2 h was preceded by augmented NE levels over some interval between time zero and time of sacrifice. As discussed above, observations of parallelism between effects of 4CIN versus NE on VMN protein profiles support the notion that the former drug treatment likely increased noradrenergic input to that site at some time point after delivery. Hindbrain metabolic substrate deficient signaling, in the absence of sensory input from other metabolic monitors (central and peripheral), may convey a state of less severe metabolic imbalance compared to systemic hypoglycemia. For instance, administration of graded insulin doses elicits divergent, dose-dependent patterns DMN, VMN, and LHA NE accumulation, likely indicative of discriminative reactivity to magnitude of hypoglycemia (Alhamami et al., 2018a). Here, 4CIN-associated reductions in NE activity may reflect distinctive communication of 'isolated' substrate shortage. It is noted that 'snap-shot' measures of NE tissue content do not shed light on how the drug treatment paradigm used here may control local catecholamine synthesis/breakdown/exocytosis ratios in each hypothalamic structure. Thus, the likelihood that 4CIN may stimulate NE neurotransmission while reducing tissue catecholamine levels in one or more locations of interest cannot be overlooked. Application of classical experimental methods involving pharmacological blockade of catecholamine synthesis or degradation would clarify effects of 4CIN on local NE release and synthesis, respectively. Given the complex neurochemical heterogeneity of individual hypothalamic structures, it is possible that 4CIN may cause dissimilar changes in noradrenergic input to distinctive neurotransmitter cell populations within a single structure. Thus, whole-nucleus measurements may obscure small local changes in NE tone that modify metabolic transmission, underscoring the ongoing need for high-resolution analytical techniques for quantification of NE input to specific neurochemical targets. AH did not alter 4CIN suppression of ARH, VMN, or DMN NE activity, but attenuated reductions in LHA NE levels in drug-treated animals, indicating that volume of lactoprivic-driven noradrenergic input to the three former structures at +2 h may be equivalent between hypoglycemia-naïve versus hypoglycemia-exposed rats. Unresolved issues that will require further investigation include possibilities that AH may impact 4CIN-controlled NE activity earlier than 2 h post-drug treatment and that equivalence of NE tissue content between insulin- versus vehicle-pretreated groups observed here may mask differential rates of matched catecholamine synthesis and release. Differential reactivity of certain hypothalamic metabolic transmitter proteins to 4CIN before compared to after AH, despite unaffected patterns of local NE activity, may reflect AH-associated alterations in lactoprivic-sensitive non-catecholaminergic input from the DVC that may exert NE-independent effects on hypothalamic neurotransmitter marker protein expression and/or or may modify reactivity of one or more of these proteins to NE.

4CIN treatment caused significant, divergent changes in circulating glucagon and corticosterone concentrations, as these counter-regulatory hormone profiles were respectively elevated or decreased by this drug. AH prevented 4CIN augmentation of glucagon release, results that imply that recurring hypoglycemia-associated negative acclimation to hindbrain lactoprivic signaling may contribute to diminished output of this critical hormone. Previous work demonstrated that DAB inhibition of VMN glycogen mobilization decreased plasma corticosterone levels alongside up-regulated VMN $GAD_{65/67}$ protein expression (Alhamami et al., 2018b). We thus speculate that hindbrain regulation of VMN glycogen metabolism and/or GABAergic transmission may govern corticosterone release. Here, AH did not modify 4CIN suppression of corticosterone. Since AH attenuated VMN $GAD_{65/67}$ and GP protein responses to this drug, it is possible that other regulatory signals of hindbrain origin may act through other hypothalamic mechanisms to inhibit this counter-regulatory hormone.

In summary, current studies investigated the hypothesis AH alters hindbrain lactoprivic control of hypothalamic metabolic neurotransmission. AH did not modify 4CIN effects on hindbrain A2 neuron catecholamine biosynthesis and nutrient transporter function, but diminished drug effects on A2 AMPK activity. Measures of hypothalamic NE content indicate that 4CIN-driven activity was generally refractory to AH over the time frame examined here. 4CIN induction of hypothalamic patterns of Fos immunostaining was suppressed by AH. Sensitivity of a subset of investigated hypothalamic metabolic neurotransmitter marker proteins was altered by AH. Other data show that AH blunted 4CIN augmentation of plasma glucagon, but did not alter drug effects on circulating glucose or corticosterone. Results identify hindbrain lactate deficiency as a stimulus for glucagon secretion, and imply that habituation of this critical counter-regulatory hormone to

recurring hypoglycemia may involve one or more hypothalamic neurotransmitters characterized here by acclimation to this critical sensory stimulus.

Acknowledgements

This research was funded by NIH DK 109382

References

Alhamami, H.N., Uddin, M.M., Mahmood, A.S.M.H., Briski, K.P., 2018a. Lateral but not medial hypothalamic AMPK activation occurs at the hypoglycemic nadir in insulin-injected male rats: impact of caudal dorsomedial hindbrain catecholamine signaling. Neuroscience 379, 103–114.

Alhamami, H.N., Alshamrani, A., Briski, K.P., 2018b. Effects of the glycogen phosphorylase inhibitor 1,4-dideoxy-1,4-imino-D-arabinitol on ventromedial hypothalamic nucleus 5′-adenosine monophosphate-activated protein kinase activity and metabolic neurotransmitter biosynthetic enzyme protein expression in eu- versus hypoglycemic male rats. Physiol. Rep. 103, 236–249.

Beverly, J.L., de Vries, M.G., Beverly, M.F., Arseneau, L.M., 2000. Norepinephrine mediates glucoprivic-induced increase in GABA in the ventromedial hypothalamus of rats. Am. J. Physiol. Regul. Integr. Comp. Physiol. 279, R990–R996.

Briski, K.P., Patil, G.D., 2005. Induction of Fos immunoreactivity labeling in forebrain metabolic loci by caudal fourth ventricular administration of the monocarboxyate transporter inhibitor, α-cyano-4-hydroxycinnamic acid. Neuroendocrinology 82, 49–57.

Briski, K.P., Koshy Cherian, A., Genabai, N.K., Vavaiya, K.V., 2009. *In situ* coexpression of glucose and monocarboxylate transporter mRNAs in metabolic-sensitive dorsal vagal complex catecholaminergic neurons: transcriptional reactivity to insulin-induced hypoglycemia and caudal hindbrain glucose or lactate repletion during insulin-induced hypoglycemia. Neuroscience 164, 1152–1160.

Chan, O., Sherwin, R., 2013. Influence of VMN fuel sensing on hypoglycemic responses. Trends Endocrinol. Metab. 24, 616–624.

Cherian, A., Briski, K.P., 2011. Quantitative RT PCR and immunoblot analyses reveal acclimated A2 noradrenergic neuron substrate fuel transporter, glucokinase, phospho-AMPK, and dopamine-beta-hydroxylase responses to hypoglycemia. J. Neurosci. Res. 89, 1114–1124.

Cryer, P.E., 2010. Hypoglycemia in type 1 diabetes mellitus. Endocrinol. Metab. Clin. N. Am. 39, 641–654.

Cryer, P.E., Davis, S.N., Shamoon, H., 2003. Hypoglycemia in diabetes. Diabetes Care 26, 1902–1912.

Hu, K.L., Chang, H.M., Li, R., Yu, Y., Qiao, J., 2019. Regulation of LH secretion by RFRP-3 - from the hypothalamus to the pituitary. Front. Neuroendocrinol. 52, 12–21.

Ibrahim, M.M.H., Alhamami, H.N., Briski, K.P., 2019. Norepinephrine regulation of ventromedial hypothalamic nucleus metabolic transmitter biomarker and astrocyte enzyme and receptor expression: role of 5′-AMP-activated protein kinase. Brain Res. 1711, 48–57.

Kale, A.Y., Paranjape, S.A., Briski, K.P., 2006. I.c.v. administration of the nonsteroidal glucocorticoid receptor antagonist, CP4-72555, prevents exacerbated hypoglycemia during repeated insulin administration. Neuroscience 140, 555–565.

Leon, S., Garcia-Galiano, D., Ruiz-Pino, F., Barroso, A., Manfredi-Lozano, M., Romero-Ruiz, A., Roa, J., Vazquez, M.J., Gaytan, F., Blomenrohr, M., van Duin, M., Pinilla, L., Tena-Sempere, M., 2014. Physiological roles of gonadotropin-inhibitory hormone signaling in the control of mammalian reproductive axis: studies in the NPFF1 receptor null mouse. Endocrinology 155, 2953–2965.

Mahmood, A.S.M.H., Bheemanapally, K., Mandal, S.K., Ibrahim, M.M.H., Briski, K.P., 2019. Norepinephrine control of ventromedial hypothalamic nucleus glucoregulatory neurotransmitter expression in the female rat: role monocarboxylate transporter function. Mol. Cell. Neurosci. 95, 51–58.

Mandal, S.K., Briski, K.P., 2018. Hindbrain dorsal vagal complex AMPK controls hypothalamic AMPK activation and metabolic neurotransmitter protein expression and counter-regulatory hormone secretion in the hypoglycemic male rat. Brain Res. Bull. 144, 171–179.

Mandal, S.K., Shrestha, P.K., Alenazi, F.S.H., Shakya, M., Alhamami, H.N., Briski, K.P., 2017. Role of hindbrain adenosine 5′-monophosphate-activated protein kinase (AMPK) in hypothalamic AMPK and metabolic neuropeptide adaptation to recurring insulin-induced hypoglycemia in the male rat. Neuropeptides 66, 25–35.

Marks, J.L., Waite, K., 1997. Intracerebroventricular neuropeptide Y acutely influences glucose metabolism and insulin sensitivity in the rat. J. Neuroendocrinol. 9, 99–103.

Müller, M.S., Pedersen, S.E., Walls, A.B., Waagepetersen, H.S., Bak, L.K., 2015. Isoform-selective regulation of glycogen phosphorylase by energy deprivation and phosphorylation in astrocytes. Glia 63, 154–162.

Nadeau, O.W., Fontes, jD, Carlson, G.M., 2018. The regulation of glycogenolysis in the brain. J. Biol. Chem. 293, 7099–7109.

Paranjape, S.A., Briski, K.P., 2005. Recurrent insulin-induced hypoglycemia causes site-specific patterns of habituation or amplification of CNS neuronal genomic activation. Neuroscience 130, 957–970.

Parikh, R., Marks, J.L., 1997. Metabolic and orexigenic effects of intracerebroventricular neuropeptide Y are attenuated by food deprivation. J. Neuroendocrinol. 9, 789–795.

Patil, G.D., Briski, K.P., 2005a. Lactate is a critical 'sensed' variable in caudal hindbrain monitoring of CNS metabolic stasis. Am. J. Physiol. Regul. Integr. Comp. Physiol. 289, R1777-R11786.

Patil, G.D., Briski, K.P., 2005b. Transcriptional activation of nucleus tractus solitarii/area postrema catecholaminergic neurons by pharmacological inhibition of caudal hindbrain mono-carboxylate transporter function. Neuroendocrinology 81, 96–102.

Sakurai, T., Amemiya, A., Ishii, M., Matsuzaki, I., Chemelli, R.M., Tanaka, H., Williams, S.C., Richardson, J.A., Kozlowski, G.P., Wilson, S., Arch, J.R., Buckingham, R.E., Haynes, A.C., Carr, S.A., Annan, R.S., McNulty, D.E., Liu, W.S., Terrett, J.A., Elshourbagy, N.A., Bergsma, D.J., Yanagisawa, M., 1998. Orexins and orexin receptors: a family of hypothalamic neuropeptides and G protein-linked receptors that regulate feeding behavior. Cell 92, 573–585.

Shakya, M., Shrestha, P.K., Briski, K.P., 2018. Hindbrain 5′-monophosphate-activated protein kinase mediates short-term food deprivation inhibition of the gonadotropin-releasing hormone-luteinizing hormone axis: role of nitric oxide. Neuroscience 383, 46–59.

Shrestha, P.K., Tanarkar, P., Ibrahim, B.A., Briski, K.P., 2014. Hindbrain medulla catecholamine cell group involvement in lactate-sensitive hypoglycemia-associated patterns of hypothalamic norepinephrine and epinephrine activity. Neuroscience 278, 20–30.

Silva, R.M., Hadjimarkou, M.M., Rossi, G.C., Pasternak, G.W., Bodnar, R.J., 2001. Beta-endorphin-induced feeding: pharmacological characterization using selective opioid antagonists and antisense probes in rats. J. Pharmacol. Exp. Ther. 297, 590–596.

van den Hoek, A.M, Voshol, P.J., Karnekamp, B.N., Buijs, R.M., Romijn, J.A., Havekes, L.M., Pijl, H., 2004. Intracerebroventricular neuropeptide Y infusion precludes inhibition of glucose and VLDL production by insulin. Diabetes 53, 2529–2534.

Van Loon, G.R., Appel, N.M., 1980. Beta-endorphin-induced increases in plasma dopamine, norepinephrine and epinephrine. Res. Commun. Chem. Pathol. Pharmacol. 27, 607–610.

Van Loon, G.R., Appel, N.M., Ho, D., 1981. Beta-endorphin-induced increases in plasma epinephrine, norepinephrine and dopamine in rats: inhibition of adrenomedullary response by intracerebral somatostatin. Brain Res. 212, 207–214.

Vavaiya, K.V., Briski, K.P., 2007. Caudal hindbrain lactate administration alters glucokinase, SUR1, and neuronal substrate fuel transporter gene expression in the dorsal vagal complex, lateral hypothalamic area, and ventromedial nucleus hypothalamus of hypoglycemic male rats. Brain Res. 1176, 62–70.

Vergoni, A.V., Bertolini, A., 2000. Role of melanocortins in the central control of feeding. Eur. J. Pharmacol. 405, 25–32.

Wardlaw, S.L., 2011. Hypothalamic proopiomelanocortin processing and the regulation of energy balance. Eur. J. Pharmacol. 660, 213–219.

Yamanaka, A., Muraki, Y., Ichiki, K., Tsujino, N., Kilduff, T.S., Goto, K., Sakurai, T., 2006. Orexin neurons are directly and indirectly regulated by catecholamines in a complex manner. J. Neurophysiol. 96, 284–298.

Yi, C.X., Serlie, M.J., Ackermans, M.T., Foppen, E., Buijs, R.M., Sauerwein, H.P., Fliers, E., Kalsbeek, K., 2009. A major role for perifornical orexin neurons in the control of glucose metabolism in rats. Diabetes 58, 1998–2005.